



UNIVERSITY OF LEEDS

This is a repository copy of *How does internal angle of hoppers affect granular flow? Experimental studies using Digital Particle Image Velocimetry.*

White Rose Research Online URL for this paper:  
<http://eprints.whiterose.ac.uk/80464/>

---

**Article:**

Antony, SJ and Albaraki, S (2014) How does internal angle of hoppers affect granular flow? Experimental studies using Digital Particle Image Velocimetry. *Powder Technology*, 268. 252 - 260. ISSN 0032-5910

<https://doi.org/10.1016/j.powtec.2014.08.027>

---

**Reuse**

Unless indicated otherwise, fulltext items are protected by copyright with all rights reserved. The copyright exception in section 29 of the Copyright, Designs and Patents Act 1988 allows the making of a single copy solely for the purpose of non-commercial research or private study within the limits of fair dealing. The publisher or other rights-holder may allow further reproduction and re-use of this version - refer to the White Rose Research Online record for this item. Where records identify the publisher as the copyright holder, users can verify any specific terms of use on the publisher's website.

**Takedown**

If you consider content in White Rose Research Online to be in breach of UK law, please notify us by emailing [eprints@whiterose.ac.uk](mailto:eprints@whiterose.ac.uk) including the URL of the record and the reason for the withdrawal request.



[eprints@whiterose.ac.uk](mailto:eprints@whiterose.ac.uk)  
<https://eprints.whiterose.ac.uk/>

# How does internal angle of hoppers affect granular flow? Experimental studies using Digital Particle Image Velocimetry

Saeed Albaraki and S. Joseph Antony\*

Institute of Particle Science and Engineering

School of Chemical and Process Engineering

University of Leeds

LS2 9JT, UK

\*Corresponding Author: [S.J.Antony@leeds.ac.uk](mailto:S.J.Antony@leeds.ac.uk), (+44 113 3432409).

## Abstract.

Mechanical behaviour of powders and grains often displays features of solid-like and liquid-like characteristics of matter. In spite of processing granular materials quite extensively in the industries, their flow behaviour is still complex to understand under different process conditions. In this paper, using Digital Particle Image Velocimetry (DPIV) and high speed videography, we probe systematically on the spatial and temporal distribution of the velocity fields of pharmaceutical excipient granules flowing through smooth hoppers with different internal (orifice) angles. This helps to visualise and identify the locations and formation of the flow channels and conversely the stagnation zones of granular materials inside the hoppers as a function of the internal angle of the hoppers. We show that even when a powder characterised as a free-flowing type in the conventional sense could experience a significant level of hindrance to flow when passing through smooth hoppers of different internal angles and its impact increases with increase in the internal angle. Theoretical predictions are made using experimentally evaluated grain-scale properties as input parameters for understanding the effects of hopper angle on the granular flow rate. A good level of agreement is obtained between the experimental and theoretical estimates of the granular flow rate in terms of the hopper angle. The outcomes presented here are a step forward in designing granular flow devices more efficiently in the future.

**Key words:** DPIV, high speed videography, hopper, granular flow, uniform flow, plough flow

## **1. Introduction**

Flow properties of granular materials for their flow from storage apparatuses and bins through different hoppers geometries are sought in several industries including pharmaceutical manufacturing, civil engineering, food processing, nuclear disposals, space engineering and powder manufacturing sectors. Though granular materials are collection of individual grains in the solid state, their mechanical behaviour is very complex and still unpredictable when compared with that of liquids and gases [1, 2]. In granular assemblies, forces are transmitted through inter-particle contacts though network-like structures referred to as force chains [3-6]. Studies show that specific signatures of strong force chains correlate to macroscopic mechanical strength characteristics of granular assemblies [5]. Recent studies using both experimental and numerical methods for the analysing stresses in static assemblies of granular media inside hopper geometries show that the hopper angle (i.e. internal angle of orifice section of hoppers through which grains discharge, Fig.1) has a strong influence on the spatial and temporal distribution of maximum shear stress distribution inside the hoppers [7].

Predicting the flow behaviours of powders and grains through storage outlets such as hoppers and silos has been of subject to detailed attention in the literatures [8-12]. In general, granular flow from storage outlets under the gravity can be broadly classified into two main divisions; mass flow and funnel flow [10, 11]. The way in which granular discharge occurs from storage outlets could lead to dramatic changes in the variation of normal and shear stress along their wall boundaries. This could subsequently affect the bulk density of granular assemblies inside their collection chambers [13]. The tendency of granular materials to form arches inside different hopper geometries during flow and the related properties such as granular jamming have been investigated extensively using both experimental and numerical methods [4, 6, 14-16]. Discrete Element Modelling (DEM) studies of granular flow [17] provide useful information on the movement of grains at both the single-grain and bulk scale levels though normally limited to studying small size flow devices for handling fine (micron-size) particles. A number of experimental techniques has been also used in the past to study the characteristics of granular flows, for example digital speckle radiography [18], gamma-ray measurements [19], electrical capacitance

tomography [20], fast X-ray tomography [21], stereo-photogrammetry [22], near infrared spectroscopy [23] and digital particle image velocimetry [24-26].

Literatures on the application of particle image velocimetry (PIV) in the field of materials processing date back to the early eighties [27]. Adrian [28] reviewed on the development of PIV and its ability to measure velocity fields of gaseous and liquid materials for a wide range of velocity. Digital particle image velocimetry (DPIV) is digital equivalent of the conventional (PIV) and laser speckle velocimetry (LSV) [28, 29]. Unlike conventional photography-based particle tracking methods, DPIV and LSV are able to provide sufficient temporal and spatial resolution of velocity fields in a defined area known as an interrogation area at multiple locations [28, 30]. In DPIV, employing a digital camera with high resolution capacities help to minimise any optical errors [29], as well as provide capabilities for post processing large quantities of experimental data such as commonly required for analysing granular flow systems. This could help to obtain non-biased results for the particle velocities from their digital records [31]. Further, in contrast to gases and liquids, applying PIV technique for granular materials does not require to use any artificial tracer particles as the grains themselves act as tracers [32]. For example, DPIV applications have been used to evaluate flow patterns of agricultural crops from silos [26, 33]. Sielamowicz et al. [26] applied DPIV to evaluate the pattern of acentric flow behaviour of grains. Sielamowicz et al. [25] successfully applied the DPIV to quantify the evolution and propagation of central flow plug zone inside 60° internal angle hopper using amaranth seeds as granular material. Application of PIV to evaluate velocity profiles of granular flow using 2-D transparent silos and hoppers have been also used in the past [25, 26, 33-36]. In these studies, the granular materials varied from agricultural seeds [25, 33] to glass beads [34]. The transparent walls were made of Plexiglas [25], Perspex [32] and clear acrylic glass [34, 35].

In summary, though a number of studies were performed in the past on probing the flow properties of granular materials, systematic level of investigations for understanding the effects of hopper angle on their flow characteristics especially in the case of pharmaceutical excipient grains is still lacking. Further, it would be desirable to complement the numerical (e.g. DEM) and theoretical predictions of granular flow characteristics using experiments, for which technologies capable of providing measurements at grain-scale resolution is required.

The present paper is aimed at addressing these key challenges together using DPIV and colour coding techniques to visualise and evaluate dynamic flow trajectories and velocity profiles within 2-D converging hopper geometries using pharmaceutical granular excipients. Also, detailed levels of experiments are conducted on the physical and mechanical properties of the grains and the walls used here.

## **2. Experiments**

### **2.1 Material and methods**

The granules used in the experiments were initially fabricated by wet granulation [37] corn starch (Sigma Aldrich, UK), which is commonly used in pharmaceutical industries as a binder, disintegrant, lubricant and bulking agent in their manufacturing processes. For this, a known quantity of starch powder was used as a raw excipient and a coloured 5% starch paste as a binder for granulating the starch. The starch paste was prepared by weighting accurately 5 gm of the corn starch powder sample and dispersed in 30 ml cold distilled water. The sample is then mixed continuously and stirred until a suspension (white colour) is developed. In another beaker, initially 70 ml of water was boiled and the suspension was then added to the boiled water in small portions with continuous mixing until a whitish and clear mucilage was developed. Subsequently, the container with the paste was subjected to a cold water bath until a thick paste was obtained. At this stage, the required colouring agent was added to the paste and stirred until the mixture became homogeneous and coloured uniformly. This procedure was repeated for preparing the pastes with different colours, so that batches of granules with different colours were also produced for experimental use later. The coloured pastes thus created were used to add into the starch excipients (38% w/w) for granulating the excipient as follows.

For the granulation process, 150 gm of corn starch powder was placed in a stainless steel tray and the coloured paste was added in small portions to the powder with continuous mixing until a dough mass was obtained. This coloured mass was pressed through a 10-mesh screen sieve to produce granules of different sizes. The granules were spread on a clean stainless steel tray and allowed to dry at room temperature for 72 hrs.

During the granulation process, no mixers (low or high shear) or heat sources were used for drying. The prepared granules were sieved using standard serial sieves. Finally, the granules (free flowing) in the size range of 300 to 1000 $\mu\text{m}$  (average diameter  $d = 650\mu\text{m}$ ) were selected for the experiments reported here. The size distribution of the granular sample used in the flow experiments are presented in Fig.2.

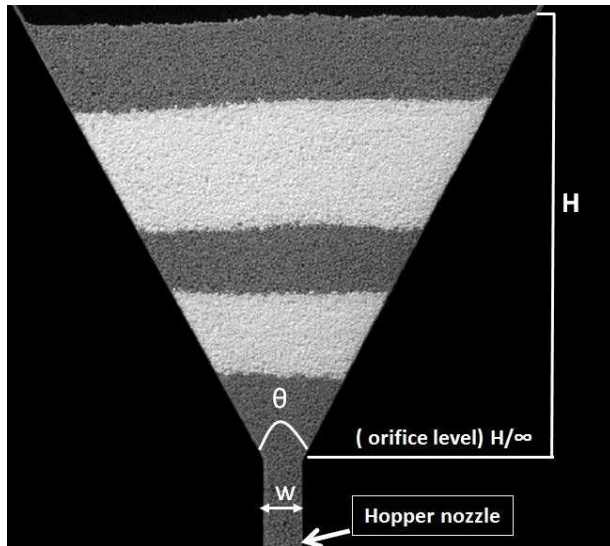


Fig.1. A typical image of granular layers filled inside the hopper ( $\theta=60^\circ$ ).

Further, standard tests were performed to characterise the physical and mechanical properties of the granules and the wall. The outcomes are summarised in table 1. The bulk and tapped density are obtained by tapped density tester. Static angle of repose is obtained by using the conventional fixed angle method while angle of internal friction, angle of wall friction and flow factors were obtained by using the ring shear cell tester (RST-XS at 5Kpa). True density was obtained by using the Helium gas Pycnometer. The obtained values of the static angle of repose, Carr's index and Hausner ratio indicate that the type of granules fabricated here is free-flowing in the conventional sense [38]. The estimated flow factor ( $ff_c$ ) value is also in the range of easy flowing grains [39]. Nevertheless, we would show later that even granules classified as generally free-flowing could experience hindrance to flow through hoppers depending on the hopper angle.

Parameter	Value
Bulk Density (g/cm <sup>3</sup> )	0.443 ± 0.004
Tapped Density(g/cm <sup>3</sup> )	0.537 ± 0.005
True Density*(g/cm <sup>3</sup> )	1.5014 ± 0.0001
Hausner Ratio	1.212
Carr's Index	17.05
Static angle of repose	(38.12) <sup>o</sup> ± 0.41
Angle of internal friction ( $\phi$ )	39 <sup>o</sup>
Angel of wall friction against Perspex ( $\phi$ )	17.9 <sup>o</sup>
Flow factor ( $ff_c$ )	4.8

Table. 1. Experimental results of the physical and mechanical properties of the granules

## 2.2 DPIV Experimental setup

To understand the effects of hopper angle on the flow properties of granular materials, we have used DPIV methodology in this study. More details on its background can be found elsewhere [25, 26, 28, 30]. Basically, the experimental setup consists of a high resolution camera using which motion of every pixel (pixel size= 137 $\mu$ m in each direction, which is lower than the size of the smallest grain used here) can be tracked during the whole period of granules discharging from different 2D hoppers considered in this study. Using a DPIV post-processing software, recorded frames (1000 frames per second of the event) of the images were analysed for mapping out the spatial and temporal distribution of velocity components during the grain movements for the whole duration of the flow.

The experimental setup consists of 2D hopper geometries made of Perspex sheets for three cases of internal angle of hopper ' $\theta$ ' ( $\theta = 30^\circ, 60^\circ$  and  $90^\circ$ ) as shown in Fig.1. The dimensions of the hoppers used here are as follow; the height (H) 8cm ( $\approx 123d$ ), orifice width (w) 7 mm ( $\approx 11d$ ), nozzle length 20 mm ( $\approx 31d$ ) and the hopper thickness (perpendicular to the plane of hopper) is 4mm ( $\approx 6d$ ). The hopper internal surfaces and edges were finely polished to minimise wall friction. The dimensions of the hopper used here follow a previous work [7]. The selected hopper dimensions, though could be viewed as relatively small in some industries, are about the size of some of the hoppers used in the grain-processing sub-stations in the space industry. We also verified that the selected dimensions

(and the ratios of the hopper dimensions to the average particle size  $d$ ) used here are adequate to maintain continuous flow during the experiments.

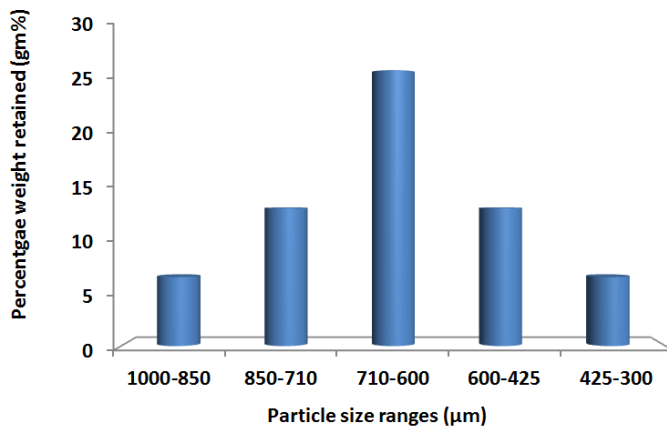


Fig.2. Particle size distribution of the granules used in the experimental study

Initially the hopper nozzle was closed to allow filling the hopper in static layers. Granular layers in different colours (Fig.1.) were built by feeding them between the Perspex sheets using a conical funnel, which was initially aligned along the central axis of the hopper. The funnel had a long flexible nozzle to help building granular layers and to minimise any segregation of the grains during filling. Layered granules also helped us to visualise and track down the flow trajectories of granules using a high speed video camera including locating any stagnation zones of granules within the hoppers as a function of the internal angle of the hoppers ( $\theta$ ) at later stages. The filling procedure for each hopper angle had been repeated for at least 15 times to ensure that the selected dimensions of the hoppers are sufficient to maintain continuous granular flow. To ensure the initial packing density of the samples, the mean weight of the granules from the different runs was calculated and the variations are within an acceptable range ( $4.503 \pm 0.191$ ,  $10.471 \pm 0.247$  and  $13.386 \pm 0.209$  gm for the  $30^\circ$ ,  $60^\circ$  and  $90^\circ$  hoppers respectively).

### 2.3 Flow Experiments

Two fluorescent lamps were used to illuminate the transparent Perspex walls of the hoppers. The positions of the lamps, light contrast and intensity were optimised to get clear images of the experimental setup without any shadow effects. By opening the hopper nozzle instantly, the flow was initiated and the entire flow process was recorded using a

high speed digital camera (Photron fastcam viewer PFV, model SA5, the speed was 1000 frame/ second, the resolution was 1024 x 1024 pixels and the maximum shutter speed is 1 $\mu$ s). DynamicStudio software platform (DSSP) was used to analyse the images frame by frame. An adaptive cross-correlation functionality built in the DSSP platform was used to analyse all of the digital frames of the grains and to calculate mean velocity vectors of the grains and their evolution during flow within the hoppers. Areas outside the hopper geometry were masked to exclude any interference and noises. Adaptive cross-correlation application iteratively adjusts the size and shape of the individual interrogation areas (IA) in order to adapt to local seeding densities and flow gradients. In the present study, the whole area of interest of the hopper is subdivided into a number of interrogation areas, each 16x16 pixels dimension.

### **3. Results and discussion**

The adaptive DPIV applied in this study is non-invasive, real time, a whole-flow-field optical measurement technique and able to provide velocity vectors of particles across the hopper width at different levels. Here we present the mean velocity vector of the grains inside the hoppers and the length of such vectors is scaled to their magnitude. Henceforth, unless mentioned otherwise, the term velocity refers to mean velocity in the following sections which is the mean of the resultant velocity for the whole duration of the flow. The coloured contours map of velocity profiles and the length of velocity vectors indicate about their spatial and temporal distributions [24, 33].

Fig.3 shows the distribution of the mean value of velocity vector within the interrogation areas of all hopper geometries considered in this study ( $\theta= 30^\circ, 60^\circ$  and  $90^\circ$ ). In general, the velocity vectors have a higher magnitude around the orifice region and along the hopper nozzle. For the case of an internal angle of the hopper equal to  $30^\circ$ , the velocity vectors generally points towards the vertical direction (downwards along the direction of the gravity), and in good agreement with previous studies reported for this case of the geometry [13, 24]. The spatial distribution of the velocity profile indicates that almost all the particles inside the  $30^\circ$  hopper are in continuous motion and the granules experience mass flow inside the hopper.

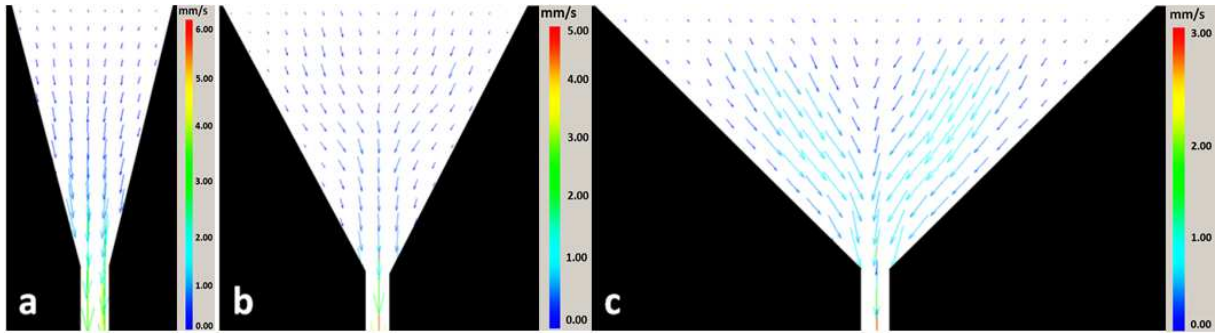


Fig.3. Distribution of mean value of resultant velocity vector profiles for granular flow through hoppers of different internal angles ( $\theta$ ): (a)  $30^\circ$  (b)  $60^\circ$  and (c)  $90^\circ$

On the other hand, the flow trend observed in the  $60^\circ$  and  $90^\circ$  internal angle hopper geometries is quite different from that of the  $30^\circ$  hopper. For higher internal angles of the hopper, the flow tends to be non-uniform in nature. For the case of  $60^\circ$  and  $90^\circ$  hoppers, the direction of the velocity vectors are mostly non-vertical inside the hoppers apart from around the orifice and nozzle regions. The extent of the angular shift in their velocity profiles increases with the internal angle of the hopper. This implies that, for such higher angle hoppers, local flow-resistance zones could form close to the wall boundaries during the flow whereas active flow occurs along the central axis - hence the flow type tends to be a funnel-flow. This is clearly evident in the case of the  $90^\circ$  hopper where dominant velocity of the flow occurs along the central axis of the hopper from the orifice level and downwards. Particles above the orifice level flow inwards and towards the central channel (channel-like central flow region). The results are in a good agreement in trends with other research work reported for the case of hopper with  $\theta = 60^\circ$  [25, 36] using amaranth seeds and black glass beads as granular materials. However, the present study provides more systematic and consistent results using a single type of starch granules across hoppers with different internal angles.

Fig.4 presents the variation of mean value of vertical velocity component at the level of hopper orifice ( $H/\infty$ , Fig.1) for the three cases of hoppers considered in this study. It is worth noting that at the orifice level ( $H/\infty$ ) of the hopper and below, the resultant velocity vectors and the vertical velocity vectors are acting along the direction of the gravity. The data was best fitted to a polynomial distribution ( $4^{\text{th}}$  order) as presented in Fig.4.

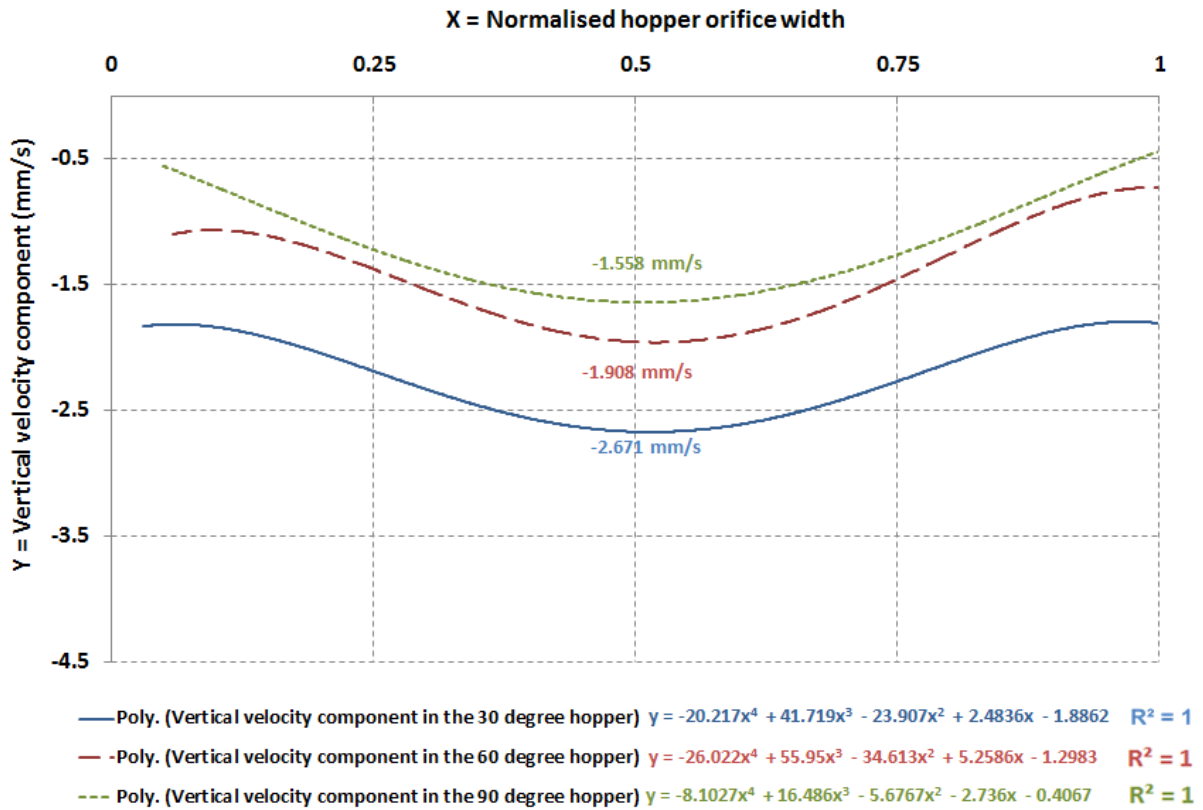


Fig. 4. Profile of vertical velocity component at hopper orifice ( $H/\infty$ ) in different hopper geometries

It is evident that the vertical velocity curves of granular flow attain almost symmetry along the central section of the hoppers. The mean vertical velocity is the highest in the case of 30° hopper angle (28.57% and 41.67% higher than that of 60° and 90° hoppers respectively). This indicates that the hopper with a relatively low internal angle (30°) tends to promote not only mass flow of grains, but also flows at relatively higher velocity across the width of the orifice. The average discharge rate of the granules from the hopper geometries were also calculated from the experiments and presented in Fig.5. The results are the mean values of eight readings for each angle and recorded in assistance with the high speed camera.

Also, the experimental results of the granular discharge rate have been compared with the theoretical results ( $W$ ) by applying Rose and Tanaka equation [40].

$$W = 0.16 D^{2.5} \rho \sqrt{g} (D/d)^{0.3} f(\alpha) (Z - 5)^{-0.5}$$

$$f(\alpha) = [\tan \frac{\theta}{2}]^{-0.35} \quad \text{if } \frac{\theta}{2} < 90 - \phi$$

$$f(\alpha) = [\tan(90 - \phi)]^{-0.35} \quad \text{if } \frac{\theta}{2} \geq 90 - \phi$$

in which D is the hopper outlet diameter,  $\rho$  is the solid bulk density, g is the gravity, d is the (average) particle diameter, Z is particle shape factor equal to 6 for the grains used here [41] and  $\alpha$  is the bulk solid static angle of repose. The comparison of both theoretical and experimental results is shown in Fig.5. The discharge rate is the highest for the lowest internal angle and decreases dramatically with an increase in the internal angle.

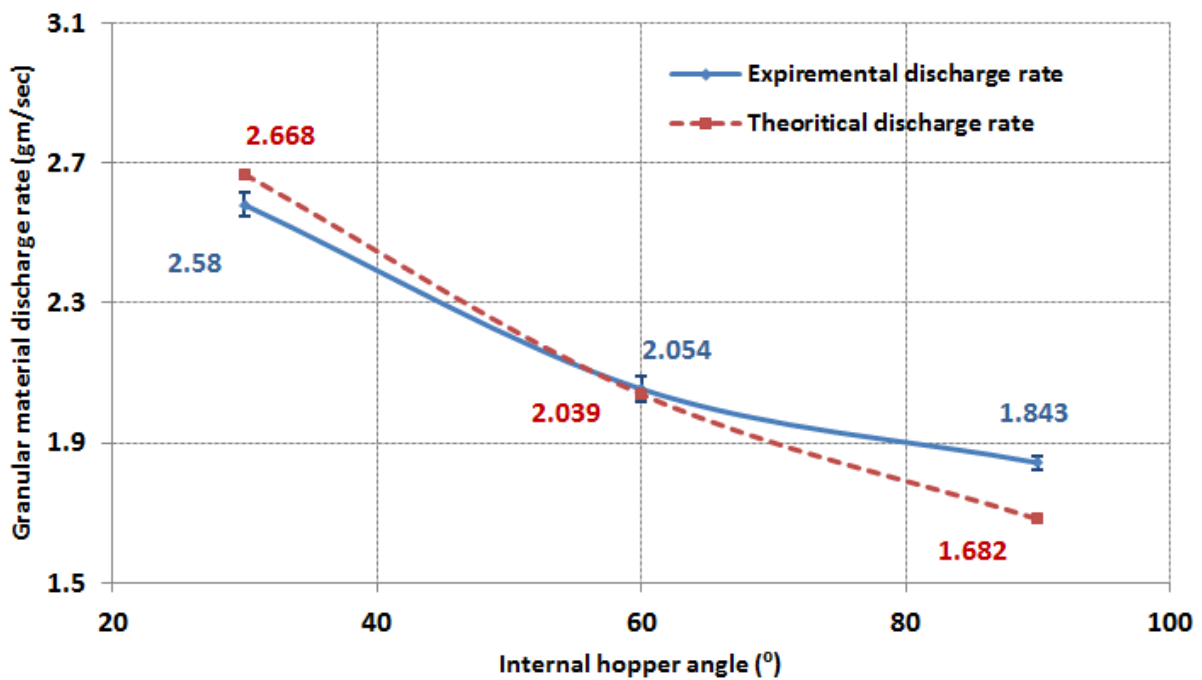


Fig. 5. Comparison of the theoretical and the experimental discharge rates at different internal hopper angle.

Also, the result shows a fairly good level of agreement between the experimental and the theoretical discharge rate for all the cases of hopper angles used here. The deviation among the experimental and theoretical results of this for the hopper angles 30°, 60° and 90° is 3.4%, 0.73% and 8.71% respectively. However, the relatively high value of deviation in the case of the 90° hopper is noted with the consideration that the theoretical prediction did not rigorously account for the complex modes of granular flow observed in the experiments especially in the case of the highest hopper angle as presented below.

In Fig.6, we present the maximum value of the vertical velocity component (i.e., occurred at the central point of the hoppers) at their orifice level ( $H/\infty$ ). The results show that the granules attain a maximum value in their vertical velocity quite rapidly since flow begins (c.a. within half of a second) and remains fairly constant for the remaining duration until the flow terminated. The flow completes first in the case of  $30^\circ$  hopper and the completion time increases with increase in internal angle of hopper in agreement with some other studies [36, 42].

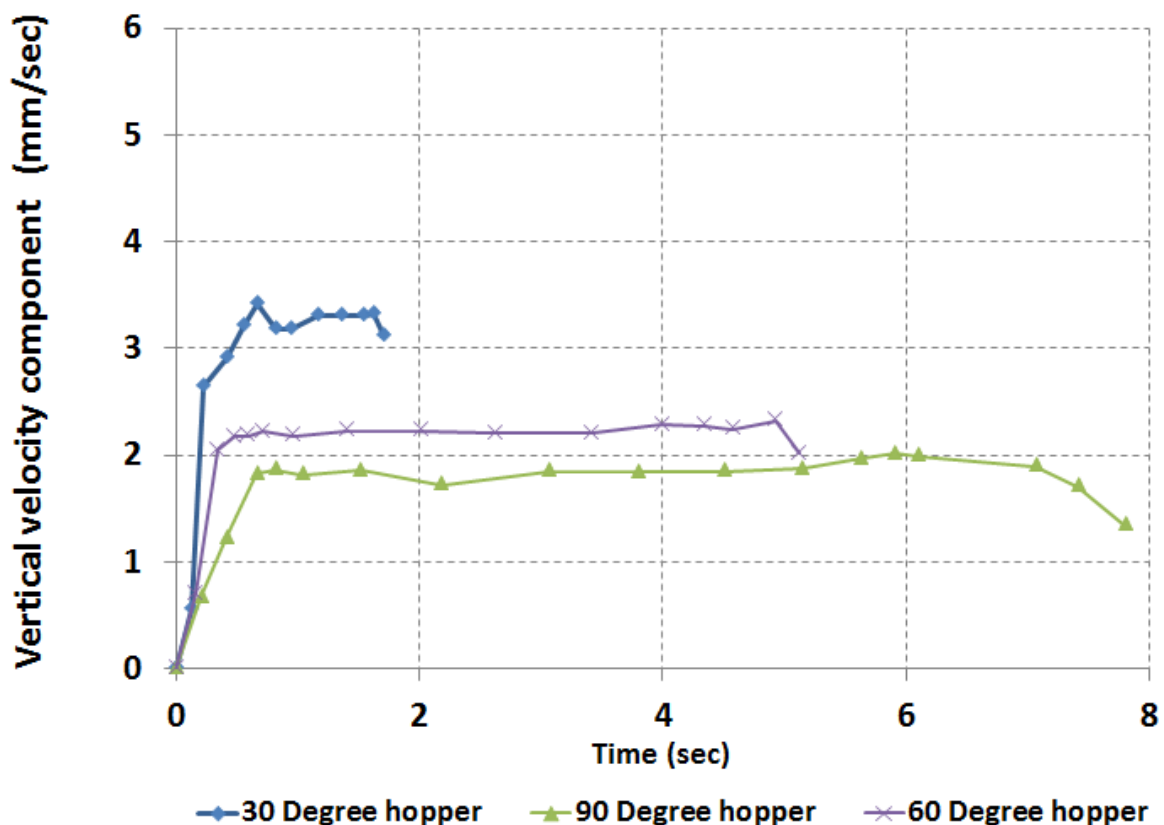


Fig. 6. Maximum value of vertical velocity component at level  $H/\infty$  in different hoppers during granular flow

Further, to examine on the influence of internal angle of the hopper on the evolution and nature of the granular discharge from hoppers, we present here the images of both the velocity vectors profile (similar to Fig.3, but presented for different time intervals) and corresponding visual images of the grains for identifying the spots of nucleation (i.e., location of initial grain dilation) and the subsequent progression of flow of the grains. These are presented in Fig.7 for the case of  $30^\circ$  hopper and in Figs. 8-11 for the case of  $60^\circ$  and  $90^\circ$

hoppers. In all of these figures, time measures marked in the images pertain to from the initiation of flow to the marked time level.

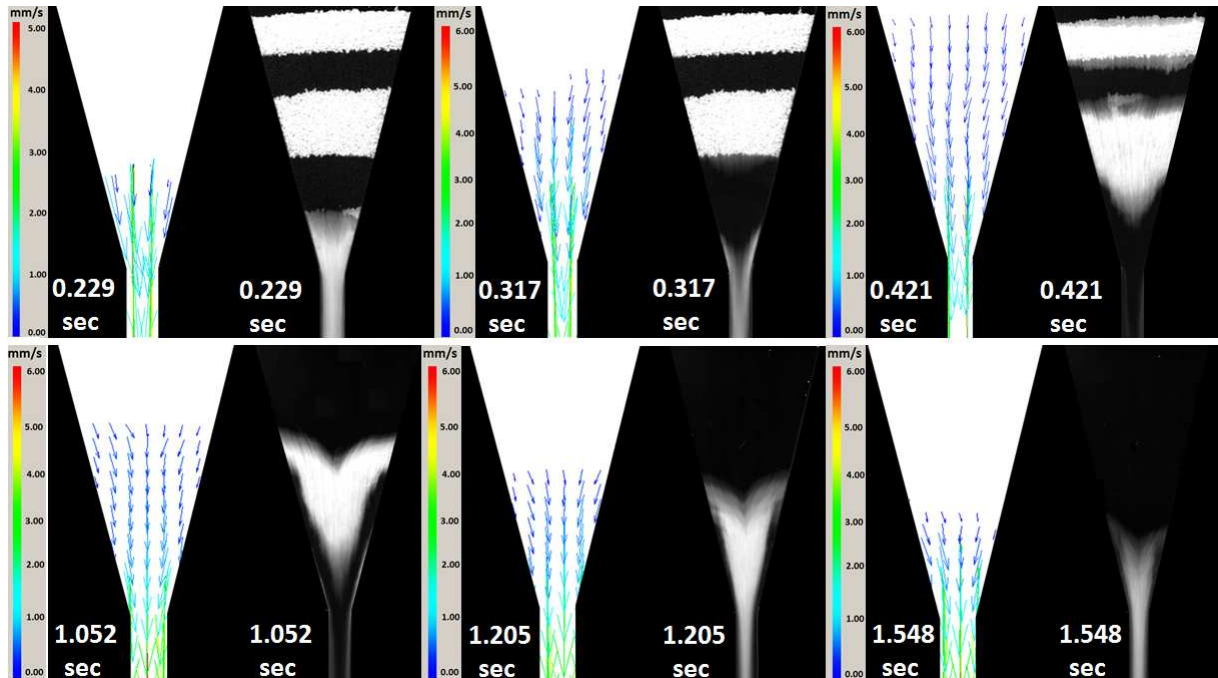


Fig.7. Mean resultant velocity vectors profiles at 30° hopper angle during different time intervals. Corresponding visual images of the granular flow are also presented here.

It is evident that, in the case of 30° hopper, the direction of the resultant velocity vectors are acting dominantly along the vertical direction (direction of gravity) at all stages of the flow. From the visual images, we observed that granular flow occurred in layers from the exit region of the hopper – i.e., ‘first in-first out’ type, implying that the initial dilation occurred at the orifice region of the hopper and the materials continued to exit in a relatively uniform manner (mass flow type). We observed this by tracking the reduction in the top level of the filling. This occurred uniformly across the width of the hopper for most periods of the flow except just prior to the end of the flow.

In the case of 60° and 90° hoppers, two distinct features of the flow were evident: at first, nucleation from the orifice region of the hopper resulted an initial plough flow and the plough extended upwards, followed by dominantly a funnel flow (combined radial and vertical motion of grains) along the central axis of the hopper (Figs.8-9). The dilation of particles in ploughs could significantly affect the granular bulk density and the wall stresses

[13]. However, in the case of 90° hopper, in addition to the above mentioned two phases (Figs.8-9), the third phase of the flow occurred mostly radially inwards indicating an avalanche trend (Fig.11).

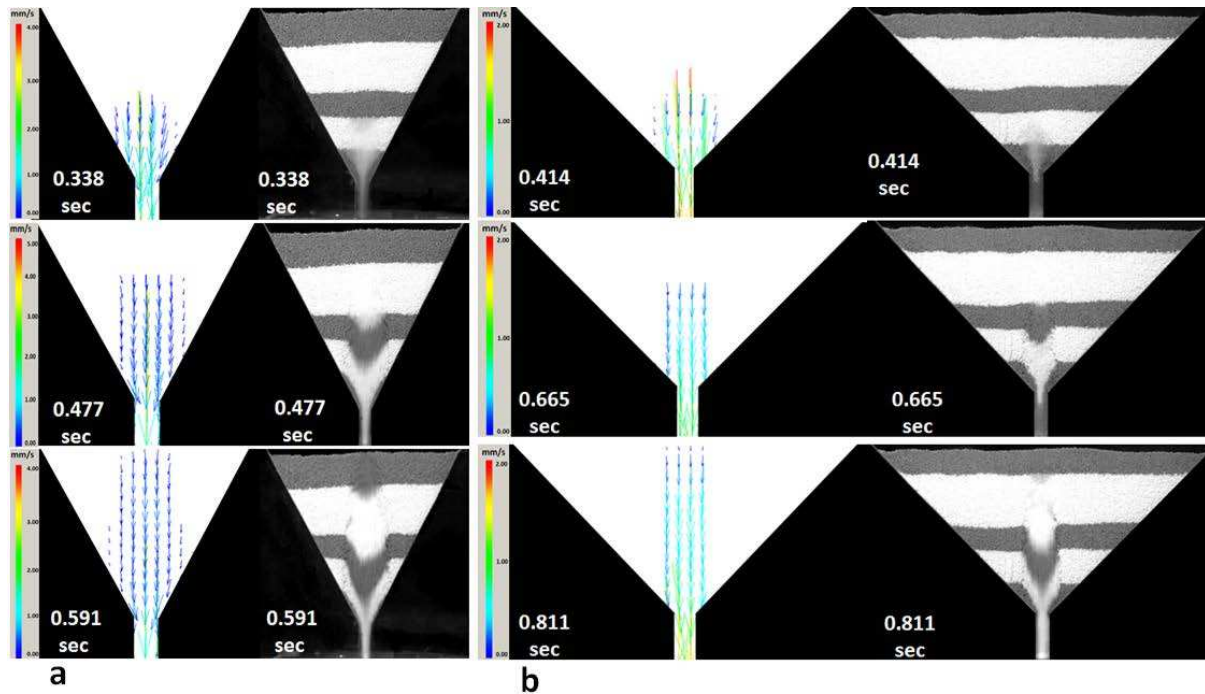


Fig.8. Mean velocity vector profiles during the first stage of the flow (formation of plough and its progression upwards): (a) 60° hopper and (b) 90° hopper. Corresponding visual images of the granular flow are also presented here

From Fig.8, it is evident that the initial plough zone gradually extended upwards while the flow of grains were dominantly along the vertical direction (direction of gravity). The length of the velocity vectors indicates a relatively high velocity of the particles at the orifice region of the hopper. The absence of velocity vectors in any other direction (other than in the vertical direction) suggests that the particles outside the plough zone were stagnant. This is further confirmed by the visual mean image at the corresponding time intervals.

Further interesting features can be observed during the second stage of the flow (Fig.9) in the case of 60° and 90° hoppers. At this stage, the previously stagnant particles close to wall boundaries now flow toward the central flow plug zone in avalanches. This is evident because the length and the magnitude of mean velocity vectors along the inner surfaces of the flow are relatively longer than those at the layers beneath. At this stage, the flow is

characterised by both the radially inward and vertical motion of the particles. The radial avalanches flow from the hopper boundaries toward the central flow plug and the vertical flow occurs along the central axis of the hopper.

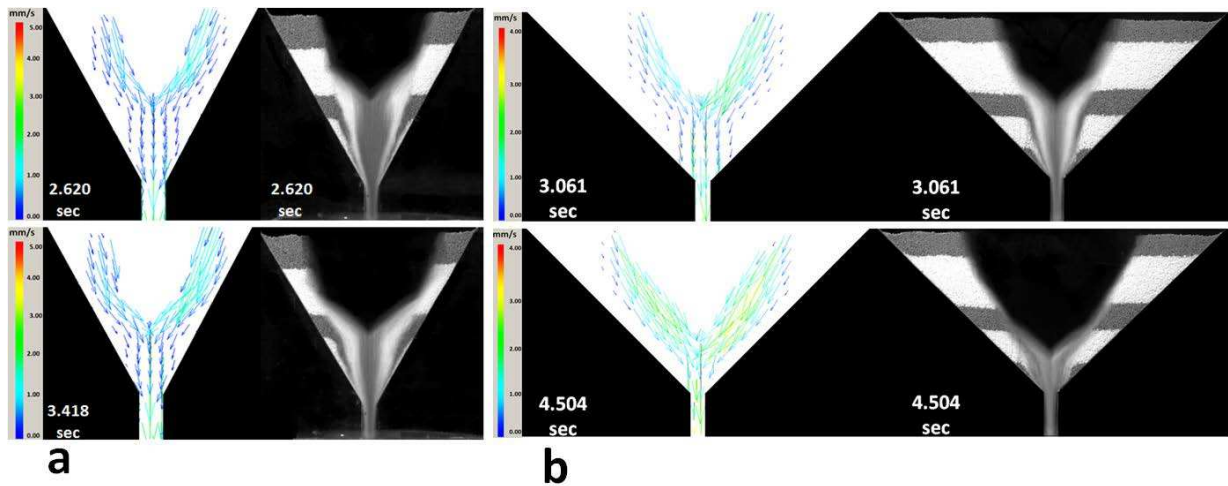


Fig.9. Mean resultant velocity vector profiles during the second stage of the flow: (a) 60° hopper and (b) 90° hopper. Corresponding visual images of the granular flow are also presented here

In the experiments, we observed that the tendency of avalanche formation is relatively higher in the case of 90° hopper. Hence for a typical case of 90° hopper, we present the velocity contour distribution map and visual image taken at an identical time duration. It is further confirmed that the flow of materials were primary through Y-shaped avalanches along their inner surfaces, while a significant amount of the stagnant materials could be observed along the wall boundaries of the Y-shaped segment (Fig.10).

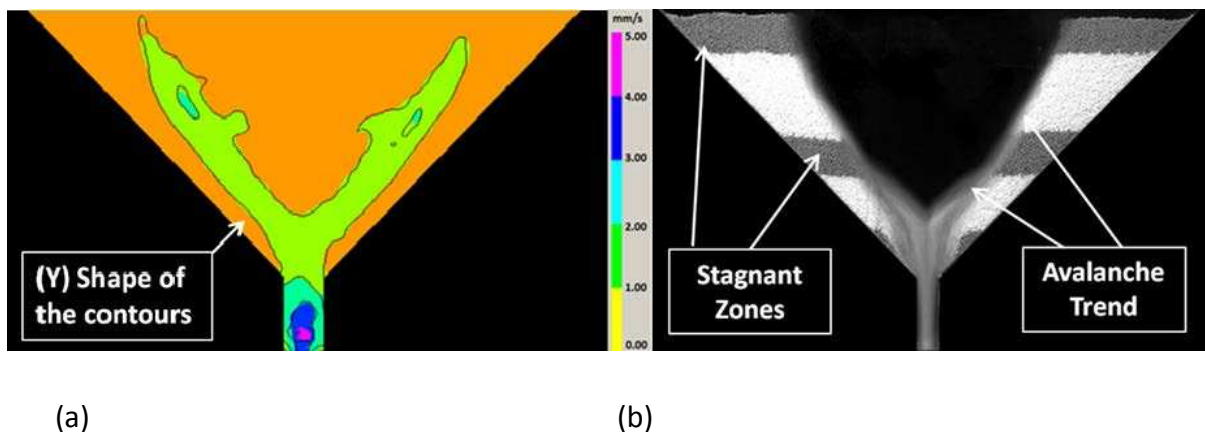


Fig.10. (a) Y-shaped map of mean resultant velocity contour and (b) visual image inside 90° geometry. Both of the images were recorded at the same time (4.504 sec).

The third stage of the flow process for the 90° hopper angle can be noted from Fig. 11. During this stage, the previously stagnant parts of the granules participate in the flow radially inwards. At this stage, generally all particles were actively participating in the flow.

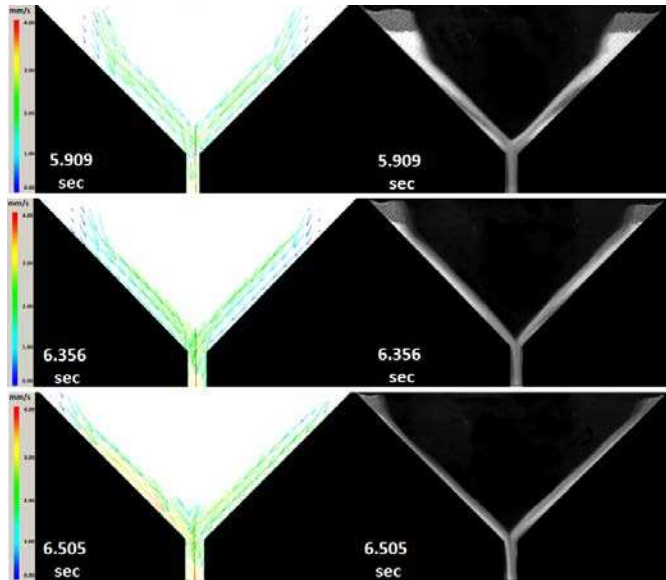


Fig.11. Mean resultant velocity vectors and flow images at the thirds phase of the flow in the case of 90° hopper angle

#### 4. Conclusion

Research progresses are reported on the flow behaviour of the pharmaceutical excipient granules through 2-D converging hopper geometries having different internal angles. The DPIV, in association with the high speed videography is shown to be an efficient methodology to measure and evaluate the velocity profiles of grains in the experiments reported here. For the case of 30° hopper angle, the flow of grains were showing mass flow trend as all granules inside the hoppers were active and in continuous motion. The mean resultant velocity vectors were acting mostly vertically (along the direction of the gravity). An increase in the hopper angle (i.e., in the case of 60° and 90° hopper angle) changed this trend from the mass flow to the funnel flow type. In general, nucleation of the flow channels tends to form nearer the orifice of the hoppers and the nucleation (plough) zone extends upwards during further flow. This mechanism results in a secondary and tertiary flow field, especially in the case of 90° hopper. During the secondary phase, granular flow is more active along the free boundaries of the grains (away from wall boundaries). During

the tertiary stage, all of the grains were flowing in avalanches radially and towards the orifice region of the hopper. These observations characterise the funnel flow type for the case of grains flowing through the hoppers with relatively higher internal angles. We have also characterised the flow properties of particles in a conventional sense using static angle of repose, Carr's index, Hausner ratio and the flow factor ( $ff_c$ ) and the results indicated that they are commonly characterised as free-flowing type. However, using the advanced measurement techniques, we report that, when such free-flowing particles flow through constrained wall boundaries, they could experience non-uniform flow and even stagnation at fairly smooth wall boundaries, which is usually associated with more cohesive and non-free flowing grains in the conventional sense. Hence care must be taken to account for the effects of actual geometrical conditions in conjunction with particle-scale properties of grains for assessing their flow performance through devices. Theoretical predictions (in which experimentally measured grain-scale input parameters are used here) for the average granular discharge rate (bulk measure) agrees fairly well with our experimental results. However, the experimental results provide an added value in terms of showing both the local and temporal distributions of the velocity field at different regimes of the granular flows. Hence the experimental results reported here on the flow properties of the granular materials could also help to bench mark future theoretical and numerical studies such as using DEM for calibrating purposes. Further studies are required to evaluate the flow behaviour of grains for higher scales of geometrical devices and describing micro-scale mechanisms of avalanches in granular flows in-terms of their particle-scale properties and geometrical conditions, for which more advancement in the related experimental technologies are also required. Evaluation of flow properties of grains with focus on non-smooth wall boundaries, density effects, industrial and other filling procedures and lubrication effects of the particles are on-going and the outcomes will be reported in the future.

## References

1. Campbell, C. S., Rapid Granular Flows. *Annual Review of Fluid Mechanics*. 22 (1990) pp. 57-92.
2. Jaeger, H. M., S. R. Nagel and R. P. Behringer, Granular solids, liquids, and gases. *Reviews of Modern Physics*. 68(4) (1996) pp. 1259-1273.
3. Majmudar, T. S. and R. P. Behringer, Contact force measurements and stress-induced anisotropy in granular materials. *Nature*. 435(7045) (2005) pp. 1079-1082.
4. Majmudar, T. S., M. Sperl, S. Luding and R. P. Behringer, Jamming transition in granular systems. *Physical Review Letters*. 98(5) (2007) .058001
5. Antony, S. J., Link between single-particle properties and macroscopic properties in particulate assemblies: role of structures within structures. *Philosophical Transactions of the Royal Society a-Mathematical Physical and Engineering Sciences*. 365(1861) (2007) pp. 2879-2891.
6. Vivanco, F., S. Rica and F. Melo, Dynamical arching in a two dimensional granular flow. *Granular Matter*. 14(5) (2012) pp. 563-576.
7. Albaraki, S., S. J. Antony and C. B. Arowosola. Visualising shear stress distribution inside flow geometries containing pharmaceutical powder excipients using photo stress analysis tomography and DEM simulations. in *AIP Conference Proceedings*. (2013), doi: 10.1063/1.4812029.
8. Jenike, A. W., Storage and flow of solids, bulletin no. 123. *Bulletin of the University of Utah*. 53(26) (1964).
9. Jenike, A. W. and J. Johanson, On the theory of bin loads. *Journal of Engineering for Industry*. 91 (1969) pp. 339-344.
10. Watson, G. R. and J. M. Rotter, A finite element kinematic analysis of planar granular solids flow. *Chemical Engineering Science*. 51(16) (1996) pp. 3967-3978.
11. Tüzün, U. and R. Nedderman, An investigation of the flow boundary during steady-state discharge from a funnel-flow bunker. *Powder Technology*. 31(1) (1982) pp. 27-43.
12. Faqih, A. N., A. W. Alexander, F. J. Muzzio and M. S. Tomassone, A method for predicting hopper flow characteristics of pharmaceutical powders. *Chemical Engineering Science*. 62(5) (2007) pp. 1536-1542.
13. Bohrnson, J. U., H. Antes, M. Ostendorf and J. Schwedes, Silo discharge: Measurement and simulation of dynamic behavior in bulk solids. *Chemical Engineering & Technology*. 27(1) (2004) pp. 71-76.
14. Jaeger, H. M. and S. R. Nagel, Physics of the granular state. *Science*. 255(5051) (1992) pp. 1523-1531.
15. Silbert, L. E., D. Ertaş, G. S. Grest, T. C. Halsey and D. Levine, Geometry of frictionless and frictional sphere packings. *Physical Review E*. 65(3) (2002). 031304.
16. O'Hern, C. S., L. E. Silbert, A. J. Liu and S. R. Nagel, Jamming at zero temperature and zero applied stress: The epitome of disorder. *Physical Review E*. 68(1) (2003) No. 011306.
17. Cleary, P. W. and M. L. Sawley, DEM modelling of industrial granular flows: 3D case studies and the effect of particle shape on hopper discharge. *Applied Mathematical Modelling*. 26(2) (2002) pp. 89-111.
18. Grantham, S. G. and F. Forsberg, Measurement of granular flow in a silo using Digital Speckle Radiography. *Powder Technology*. 146(1-2) (2004) pp. 56-65.
19. Tan, S. and T. Fwa, Influence of voids on density measurements of granular materials using gamma radiation techniques. *Geotechnical Testing Journal*. 14(3) (1991) pp. 257-265.

20. Grudzień, K., E. Maire, J. Adrien and D. Sankowski, Analysis of funnel flow in rectangular silo based on ECT data. *Nature*. 5 (12) (2010) pp. 681-694.
21. Baxter, G., R. Behringer, T. Fagert and G. Johnson, Pattern formation and time-dependence in flowing sand, in *Two phase flows and waves*, Springer .(1990) pp. 1-29.
22. Desrues, J. and G. Viggiani, Strain localization in sand: an overview of the experimental results obtained in Grenoble using stereophotogrammetry. *International Journal for Numerical and Analytical Methods in Geomechanics*. 28(4) (2004) pp. 279-321.
23. Sarraguca, M. C., A. V. Cruz, S. O. Soares, H. R. Amaral, P. C. Costa and J. A. Lopes, Determination of flow properties of pharmaceutical powders by near infrared spectroscopy. *Journal of Pharmaceutical and Biomedical Analysis*. 52(4) (2010) pp. 484-492.
24. Ostendorf, M. and J. Schwedes, Application of Particle Image Velocimetry for velocity measurements during silo discharge. *Powder Technology*. 158(1-3) (2005) pp. 69-75.
25. Sielamowicza, I., S. Blonski and T. A. Kowalewski, Digital particle image velocimetry (DPIV) technique in measurements of granular material flows, Part 2 of 3-converging hoppers. *Chemical Engineering Science*. 61(16) (2006) pp. 5307-5317.
26. Sielamowicz, I., M. Czech and T. A. Kowalewski, Empirical analysis of eccentric flow registered by the DPIV technique inside a silo model. *Powder Technology*. 212(1) (2011) pp. 38-56.
27. Adrian, R. J., Scattering particle characteristics and their effect on pulsed laser measurements of fluid flow: speckle velocimetry vs particle image velocimetry. *Applied Optics*. 23(11) (1984) pp. 1690-1691.
28. Adrian, R. J., Particle-imaging techniques for experimental fluid mechanics. *Annual Review of Fluid Mechanics*. 23(1) (1991) pp. 261-304.
29. Willert, C. and M. Gharib, Digital particle image velocimetry. *Experiments in Fluids*. 10(4) (1991) pp. 181-193.
30. Adrian, R. J., Twenty years of particle image velocimetry. *Experiments in Fluids*. 39(2) (2005) pp. 159-169.
31. Westerweel, J., Theoretical analysis of the measurement precision in particle image velocimetry. *Experiments in Fluids*. 29(1) (2000) pp. S003-S012.
32. Slominski, C., M. Niedostatkiewicz and J. Tejchman, Application of particle image velocimetry (PIV) for deformation measurement during granular silo flow. *Powder Technology*. 173(1) (2007) pp. 1-18.
33. Sielamowicz, I., S. Blonski and T. A. Kowalewski, Optical technique DPIV in measurements of granular material flows, Part 1 of 3 - plane hoppers. *Chemical Engineering Science*. 60(2) (2005) pp. 589-598.
34. Lueptow, R., A. Akonur and T. Shinbrot, PIV for granular flows. *Experiments in Fluids*. 28(2) (2000) pp. 183-186.
35. Chou, C. S., J. Smid and R. Y. Chen, Flow patterns and stresses on the wall in a two-dimensional flat-bottomed bin. *Journal of the Chinese Institute of Engineers*. 26(4) (2003) pp. 397-408.
36. Choi, J., A. Kudrolli and M. Z. Bazant, Velocity profile of granular flows inside silos and hoppers. *Journal of Physics-Condensed Matter*. 17(24) (2005) pp. S2533-S2548.
37. Kristensen, H. G. and T. Schaefer, Granulation: A review on pharmaceutical wet-granulation. *Drug development and industrial pharmacy*. 13(4-5) (1987) pp. 803-872.
38. The United States Pharmacopeia and National Formulary (USP 29-NF24).<1174> Powder flow. United States Pharmacopeial Convention, 2007
39. Schwedes, J., Review on testers for measuring flow properties of bulk solids (based on an IFPRI-Report 1999). *Granular Matter*. 5(1) (2003) pp. 1-43.
40. Rose, H. and T. Tanaka, Rate of discharge of granular materials from bins and hoppers. *The Engineer*. 208 (1959) pp. 465-469.

41. Heywood, H., Calculation of the Specific Surface of a Powder. Proceedings of the Institution of Mechanical Engineers. 125(1) (1933) pp. 383-459.
42. Alonso-Marroquin, F., S. I. Azeezullah, S. A. Galindo-Torres and L. M. Olsen-Kettle, Bottlenecks in granular flow: When does an obstacle increase the flow rate in an hourglass? Physical Review E. 85(2) (2012) No. 020301(R).